

Entanglement of elastic and inelastic scattering

Gerald A. Miller *Department of Physics, University of Washington, Seattle, Washington 98195-1560, USA*

(Received 18 July 2023; accepted 28 September 2023; published 11 October 2023)

The entanglement properties of systems in which elastic and inelastic reactions occur in projectile-target interactions is studied. A new measure of entanglement, the scattering entropy, based on the unitarity of the S matrix (probability conservation), is suggested. Using simple models for both low- and high-energy interactions, the amount of entanglement is found to track with the strength of the inelastic interaction. The familiar example of the classical “black disk,” or total absorption, model is found to correspond to maximum entanglement. An analysis of high-energy pp scattering data shows that entanglement is near maximum for laboratory energies greater than about 1 GeV, showing that the total absorption model is a reasonable starting point for understanding the data.

DOI: [10.1103/PhysRevC.108.L041601](https://doi.org/10.1103/PhysRevC.108.L041601)

Introduction. The implications of entanglement in quantum mechanics and quantum field theory have recently been studied in many papers. For a long list of recent references see Ref. [1]. This new interest has been stimulated by the connection with quantum computing. Work related to hadron, QCD, and Electron-Ion Collider (EIC) physics appears in Refs. [2–7]. The entanglement properties of nucleon-nucleon scattering and nucleon-nucleus elastic scattering are discussed in Refs. [8–12]. The connections between entanglement and nuclear structure are presented in [13–21]. There is also a possible deep connection between entanglement and underlying symmetries of the standard model [8–11,22].

The present Letter is concerned with situations in which a projectile can excite a target. One of the challenges in studying entropy and entanglement for scattering is the need to develop proper definitions for the necessary infinite-dimensional Hilbert space. This is done here using the requirements of unitarity.

A special and somewhat ubiquitous case is the scattering of a particle from a totally absorbing “black disk” of radius R [23–25]. This situation approximately occurs in low-energy α -nucleus scattering and in high-energy proton-proton scattering. In the total absorption limit, following the requirement of unitarity of the S matrix, the elastic σ_{el} and inelastic σ_{inel} cross sections are equal. The inelastic cross section is πR^2 , so that the total cross section is $2\pi R^2$, twice the geometric cross section. I will argue that when $\sigma_{el} = \sigma_{inel}$ the entanglement entropy is maximized.

Low-energy projectile-target scattering and a new measure of entropy. Consider projectile-target scattering at energies sufficiently low so that there is only s -wave scattering. Furthermore, the model definition is that there is only inelastic scattering to a single excited state, X . I consider examples in which the inelastic scattering ranges from relatively small, corresponding, for example, to neutron-nucleus scattering, to relatively large, corresponding to alpha-nucleus scattering. Another example, discussed below, is nucleon-nucleon

scattering in which interactions cause either the target or projectile to be in an excited state.

The initial state is a product of a plane wave state and the target ground state, G . As a product state there is no entanglement. Interactions occur such that after the scattering event the projectile-target wave function is given by

$$|\Psi\rangle = |u_1\rangle \otimes |G\rangle + |u_2\rangle \otimes |X\rangle, \quad (1)$$

where $|u_1\rangle$ represents a projectile with energy corresponding to elastic scattering and $|u_2\rangle$ represents a projectile with an energy corresponding to inelastic scattering. Measurement of the energy of the projectile determines whether or not the nucleus is in its ground or excited state. Thus the state represented by Eq. (1) is an entangled state. The next step is to work out a way to calculate entanglement properties. The wave function, $|\Psi\rangle$, is almost of the form of the Schmidt decomposition in which the different coefficients represent probability amplitudes. Here the wave functions are in the continuum, so that discrete normalization conventions are not applicable. It seems necessary to develop a new method to compute entropy.

I use an exactly soluble model [26] to illustrate and develop the necessary formalism. I argue below that the formalism is more general than the model. In this model the interactions are represented by delta-shell interactions [25] that can be thought of as approximating interactions at the surface of the target. Then the radial wave functions $u_{1,2}(r)$ satisfy the coupled-channels equations:

$$d^2u_1/dr^2 + [k^2 - V_1\delta(r-a)]u_1 = V_{12}\delta(r-a)u_2, \quad (2)$$

$$d^2u_2/dr^2 + [k^2 - \Delta^2 - V_2\delta(r-a)]u_2 = V_{21}\delta(r-a)u_1. \quad (3)$$

Hermiticity demands $V_{12} = V_{21}$, and calculations are limited to the case $V_1 \neq 0$, $V_{12} \neq 0$, $V_2 = 0$ to gain analytic insight. The parameter Δ is proportional to the energy difference between the excited and ground states. The solution of Eq. (2)

for u_1 is expressed in terms of the free-particle Green's function $g_1(r, r')$ as

$$u_1(r) = \frac{\sin kr}{k} + V_1 g_1(r, a) u_1(a) + V_{12} g_1(r, a) u_2(a), \quad (4)$$

with

$$g_1(r, r') = -(1/k) \sin kr_{<} e^{ikr_{>}}, \quad (5)$$

$r_{<}$ ($r_{>}$) is the smaller (larger) of (r, r') . The solution of Eq. (3) for u_2 is given by

$$u_2(r) = g_2(r, a) V_{21} u_1(a) \quad (6)$$

with

$$g_2(r, r') = -(1/k_2) \sin k_2 r_{<} e^{ik_2 r_{>}}, \quad (7)$$

where $k_2 \equiv \sqrt{k^2 - \Delta^2}$. The results for $u_{1,2}(r)$ express the condition that the initial state is a plane wave incident on the ground state of the target nucleus. The use of Eq. (6) in Eq. (4) leads to the result

$$u_1(r) = (1/k) \sin kr + T_{11} e^{ikr} \quad (8)$$

for $r > a$, with the T -matrix element given by

$$T_{11} = \frac{\left(\frac{\sin ka}{k}\right)^2 [V_1 + V_{12}^2 g_2(a, a)]}{1 - [V_1 + V_{12}^2 g_2(a, a)] g_1(a, a)}. \quad (9)$$

The relation between T_{11} and the complex-valued scattering phase shift, δ_0 , is given by

$$T_{11} = \frac{e^{2i\delta_0} - 1}{2ik}. \quad (10)$$

Similarly

$$u_2(r) = T_{12} e^{ik_2 r}, \quad (11)$$

with

$$T_{12} = \frac{V_{12} \left(\frac{\sin ka}{k}\right) \left(\frac{\sin k_2 a}{k_2}\right)}{1 - [V_1 + V_{12}^2 g_2(a, a)] g_1(a, a)}. \quad (12)$$

Next, I turn to the entanglement properties of the model. The textbook definition is the entanglement entropy, the von Neumann entropy, given by $S = -\text{Tr}[\rho \log_2 \rho]$, where ρ is the one-body density matrix. This is typically evaluated by diagonalizing ρ in a discrete basis. Here continuum wave functions, normalized as delta functions, are used. So there is a need to obtain an appropriate definition of probability. This is done through the optical theorem, an expression of the unitarity of the S matrix:

$$\sigma_{\text{tot}} = \frac{4\pi}{k} \text{Im}[T_{11}]. \quad (13)$$

The left-hand side is sum of the elastic and inelastic scattering cross sections, integrated over all angles. The result for the present model is expressed as

$$1 = \frac{k|T_{11}|^2 + k_2|T_{12}|^2}{\text{Im}[T_{11}]}, \quad (14)$$

a relation that can be checked numerically using Eqs. (9) and (12) for T_{11} and T_{12} . Equation (14) leads to a natural definition of probabilities based on the number of counts detected at an

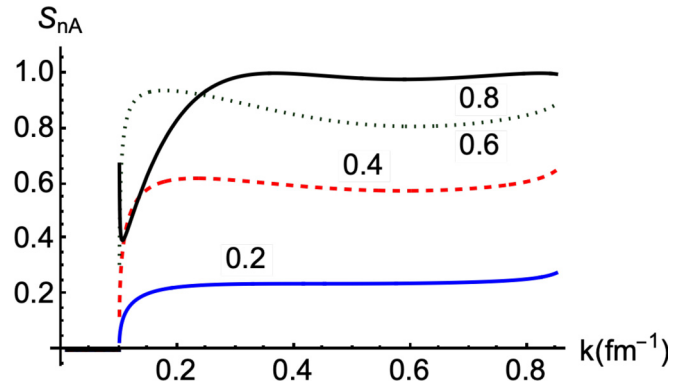


FIG. 1. S_{nA} as a function of k for the four different values of V_{12}/V_1 shown in the figure.

asymptotically located detector. The ground state probability P_G is given by

$$P_G = \frac{k|T_{11}|^2}{\text{Im}[T_{11}]} \quad (15)$$

and the excited state probability P_X is given by

$$P_X = \frac{k_2|T_{12}|^2}{\text{Im}[T_{11}]}, \quad (16)$$

and, via Eq. (14), $P_G + P_X = 1$.

Therefore, one may define the projectile-target (pT) entanglement entropy S_{pT} of the final state as

$$S_{pT} = -P_G \ln_2 P_G - P_X \ln_2 P_X. \quad (17)$$

This entanglement entropy, termed the *scattering entropy*, is minimized if either of P_G or P_X vanishes. In that case the final scattering state is a simple tensor product. The scattering entropy is maximized at $S_{pT} = 1$ when $P_G = P_X$. Using unitarity to define the entanglement entropy avoids the need to introduce infinite volume factors and the need to regularize them, as found in [27,28]. Figure 1 shows S_{pT} for parameters $a = 3.5$ fm, $V_1 = 0.25$ fm $^{-1}$ for different ratios V_{12}/V_1 as a function of k the incident momentum. The parameter $\Delta = 0.1$ fm $^{-1}$. The situation of $V_{12}/V_1 = 0.2$ is similar to that of neutron-nucleus interactions in which the inelastic scattering is relatively small. The stronger absorption situation of $V_{12}/V_1 = 1$ is similar to that of alpha-nucleus interactions in which the inelastic scattering is large. Note also that Eq. (9) shows that T_{11} is periodic in k and vanishes whenever $ka = n\pi$.

For values of $k < \Delta$ the entanglement entropy vanishes because the target cannot be excited. For higher values the scattering entropy is at its maximum value when $V_{12}/V_1 = 1$. This result can be understood directly from Eqs. (15) and (16). If $V_1 = V_2$ these quantities are approximately equal if $V_1/k \ll 1$ and $k \gg \Delta$. This result is similar to that of the total absorption model in which the elastic and inelastic cross sections are the same. But here there is only one phase shift. The unusual cusplike near-threshold behavior for the case when $V_{12}/V_1 = 1$ arises from the nonanalytic square root behavior of k_2 combined with the increasing importance of the second term in the numerator of Eq. (9).

The key lesson of Fig. 1 is that entanglement entropy, as measured by the scattering entropy, increases as the tendency for inelastic scattering increases.

High-energy scattering in a two-channel model. The scattering wave function $|\Psi\rangle$ is given again by Eq. (1). In the high-energy limit the wave number k is large compared to the inverse size of the system and large compared to the energy difference between the ground and excited states represented by Δ . Thus Δ is neglected in solving the relevant wave equations, but kept nonzero but very small, to maintain the entanglement property that measuring energy of the projectile in the final state determines whether or not the target remains in the ground state.

The coupled-channel equations for high-energy scattering are then given by

$$\nabla^2 \psi_1 + (k^2 - V)\psi_1 = U\psi_2, \quad (18)$$

$$\nabla^2 \psi_2 + (k^2 - V)\psi_2 = U\psi_1. \quad (19)$$

The implementation of the eikonal or short-wavelength approximation is made by using $\psi_{1,2}(\mathbf{r}) = e^{ikz}\phi_{1,2}(\mathbf{b}, z)$ in which the direction of the beam is denoted as \hat{z} and the direction transverse to that by \mathbf{b} . The procedure [29] is to use these in the coupled-channel equations and with large k neglect the terms $\nabla^2 \phi_{1,2}$. This approximation is valid under two conditions [29]: (i) the short-wavelength limit that $1/k$ is less than any distance scale in the problem, and (ii) $(V, U)/k^2 \ll 1$ to prevent backscattering. Then the coupled-channel equations become

$$2ik \frac{\partial \phi_1}{\partial z} - V\phi_1 = U\phi_2, \quad (20)$$

$$2ik \frac{\partial \phi_2}{\partial z} - V\phi_2 = U\phi_1. \quad (21)$$

Let $\phi \equiv \phi_1 + \phi_2$ and $\chi \equiv \phi_1 - \phi_2$. Adding the two equations gives

$$2ik \frac{\partial \phi}{\partial z} = (U + V)\phi, \quad (22)$$

and subtracting the two gives

$$2ik \frac{\partial \chi}{\partial z} = (V - U)\chi \quad (23)$$

with solutions

$$\phi(\mathbf{b}, z) = \exp \left[\frac{-i}{2k} \int_{-\infty}^z dz' [V(\mathbf{b}, z') + U(\mathbf{b}, z')] \right] \quad (24)$$

$$\chi(\mathbf{b}, z) = \exp \left[\frac{-i}{2k} \int_{-\infty}^z dz' [V(\mathbf{b}, z') - U(\mathbf{b}, z')] \right]. \quad (25)$$

The two-component scattering amplitude is given by

$$\hat{f}(\mathbf{k}', \mathbf{k}) = \frac{-1}{4\pi} \int d^3r e^{-ik' \cdot \mathbf{b}} \begin{bmatrix} V & U \\ U & V \end{bmatrix} \begin{bmatrix} \phi_1 \\ \phi_2 \end{bmatrix}, \quad (26)$$

with the upper element of \hat{f} , f_G , corresponding to elastic scattering and the lower element, f_X , to inelastic scattering.

Then evaluation leads to the results

$$f_G(\mathbf{k}', \mathbf{k}) = \frac{ik}{2\pi} \int d^2b e^{-ik' \cdot \mathbf{b}} (1 - e^{-i\delta_V(\mathbf{b})} \cos \delta_U(\mathbf{b})), \quad (27)$$

$$f_X(\mathbf{k}', \mathbf{k}) = \frac{-k}{2\pi} \int d^2b e^{-ik' \cdot \mathbf{b}} e^{-i\delta_V(\mathbf{b})} \sin \delta_U(\mathbf{b}), \quad (28)$$

where

$$\delta_V \equiv \frac{1}{2k} \int_{-\infty}^{\infty} dz' V(\mathbf{b}, z'), \quad \delta_U \equiv \frac{1}{2k} \int_{-\infty}^{\infty} dz' U(\mathbf{b}, z'). \quad (29)$$

The evaluation of entanglement entropy requires an understanding of unitarity. The statement of unitarity via the optical theorem is

$$\sigma_{Tot} = \int d\Omega (|f_G|^2 + |f_X|^2) = \frac{4\pi}{k} \text{Im}[f_G(\mathbf{k}', \mathbf{k})], \quad (30)$$

a relationship that must be checked within the current model. Taking the imaginary part of Eq. (27) yields

$$\text{Im}[f_G(\mathbf{k}, \mathbf{k})] = \frac{k}{2\pi} \int d^2b [1 - \cos \delta_V(\mathbf{b}) \cos \delta_U(\mathbf{b})]. \quad (31)$$

The evaluation of the angular integrals of $|f_{G,X}|^2$ may be done using an approximation, valid when the eikonal approximation is valid, namely [29]

$$\int d\Omega e^{ik' \cdot (\mathbf{b} - \mathbf{b}')} \approx 2\pi \frac{1}{k^2 b} \delta(b - b'). \quad (32)$$

Using this leads to the results

$$\begin{aligned} \int d\Omega |f_G(\mathbf{k}', \mathbf{k})|^2 &= \int d^2b (1 - 2 \cos \delta_V \cos \delta_U + \cos^2 \delta_U), \\ \int d\Omega |f_X(\mathbf{k}', \mathbf{k})|^2 &= \int d^2b \sin^2 \delta_U, \end{aligned} \quad (33)$$

so that the validity of Eq. (30) is maintained. Therefore unitarity may again be used to define the eikonal probabilities, $P_{G,X}^e$:

$$P_G^e = \frac{\int d^2b [1 - 2 \cos \delta_V(b) \cos \delta_U(b) + \cos^2 \delta_U(b)]}{2 \int d^2b [1 - \cos \delta_V(b) \cos \delta_U(b)]} \quad (34)$$

$$P_X^e = \frac{\int d^2b \sin^2 \delta_U(b)}{2 \int d^2b [1 - \cos \delta_V(b) \cos \delta_U(b)]}, \quad (35)$$

and

$$S^e = -P_G^e \ln_2 P_G^e - P_X^e \ln_2 P_X^e. \quad (36)$$

The case with $U = \pm V$ yields $P_G^e = P_X^e = 1/2$, and a maximum of entropy. This is similar to the total absorption limit in which elastic and inelastic cross sections are equal. This means that the black disk limit corresponds to maximum scattering entropy.

Presenting a brief discussion of the total absorption limit is worthwhile. The partial wave decomposition of the scattering amplitude $f(\theta)$ for a spinless particle is

$$f(\theta) = \frac{-i}{2k} \sum_l (2l+1)(\eta_l - 1) P_l(\cos \theta). \quad (37)$$

The strong absorption model is defined by $\eta_l = 0$ for $l \leq L$ and $\eta_l = 1$ for $l > L$, with $L \approx kR$. The sum is then given by

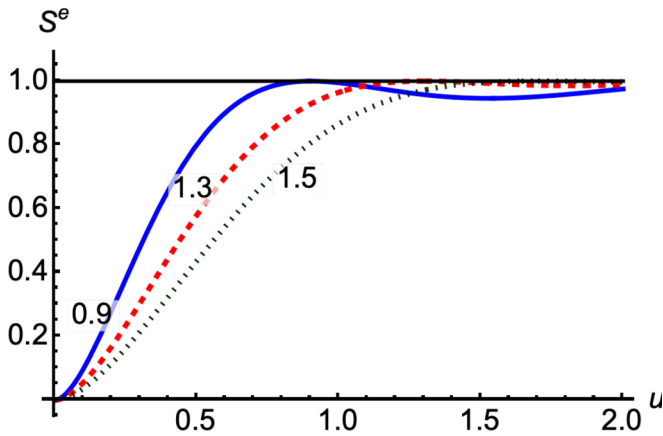


FIG. 2. S^e as a function of the dimensionless variable u for the three different values of v . The values of v are 0.9 (solid), 1.3 (dashed), and 1.5 (dotted). These values correspond to total cross sections of 22, 40, and 56 mb for $u = v$.

$f(\theta) \approx \frac{i}{k} L(L+1) \frac{J_1(L\theta)}{L\theta}$, a form familiar from Fraunhofer diffraction. In nuclear physics this is known as the Blair model [30,31]. Data were reproduced, for example [32] using a distribution without a sharp edge, $\eta_l = 1/[1 + \exp(L-l)/b]$ with $b > 1/2$. This is a grey disk model.

To see if the total absorption or grey disk model is a result of the present calculation, I provide a specific example, based on parameters typical of proton-proton scattering, and use a Gaussian density $\rho(r) = \exp[-r^2/R^2]$, where R is the radius parameter, taken here as $\sqrt{2}$ fm obtained by convoluting Gaussian densities (radius parameter 1 fm) of two protons. Then let $V(r) = V_0\rho(r)$ and $U(r) = U_0\rho(r)$. I treat the interactions as coming from vector exchanges—the typical treatment of high-energy hadron-hadron scattering [33,34]. Thus I use constants $\lambda_{U,V}$ defined as $V_0 \equiv 2\lambda_V k$ and $U_0 \equiv 2\lambda_U k$ so that evaluation of Eq. (29) yields the results $\delta_{V,U}(b) = \lambda_{V,U} \sqrt{\pi} R \exp(-b^2/R^2)$. The value of scattering entropy is then independent of energy for sufficiently high energies. Using Eq. (30) with values of $\lambda_V = \lambda_U$ of about 100 MeV gives a total cross section of about 40 mb, the typical value of the high-energy, proton-proton cross section.

The results, independent of the signs of U_0 and V_0 , are shown in Fig. 2 in terms of $u \equiv \lambda_U \sqrt{\pi} R$ and $v \equiv \lambda_V \sqrt{\pi} R$. Maximum entanglement is reached, as expected from Eqs. (34) and (35), for cases with $u = v$. Observe that, except for very small values of u (small inelastic scattering) the entanglement entropy is always substantial.

It is useful to learn if the results of the present calculation correspond to the total absorption or gray disk model. To do this, refer to Eq. (27) and define $\eta(b) \equiv e^{-i\delta_V(b)} \cos \delta_U(b)$. This quantity is shown in Fig. 3 for the case $u = v = 1.3$. The present calculation is seen to correspond to the grey disk model, not far from the total absorption model.

Extension to more than one excited state and a general result. Can the models of the previous two models be extended to include more than one excited state? What then can one say about entanglement? If there is more than one excited state, a single measurement of the projectile energy cannot be used

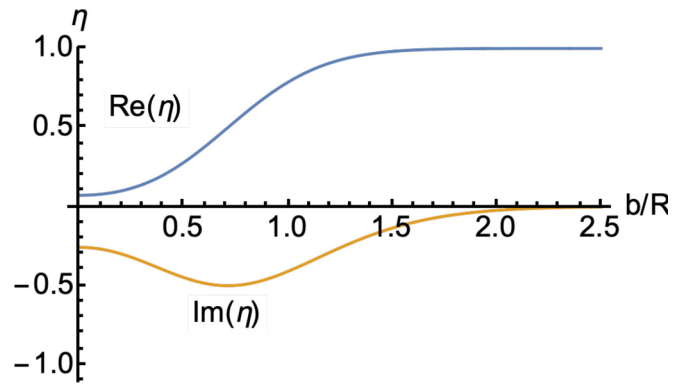


FIG. 3. Real and imaginary parts of $\eta(b)$.

to determine the specific excited state of the target. This is because the final state might have two particles in the continuum, leading to degeneracies in which different continuum and bound state energies have the same total sum. In that case, the entanglement properties are then unknown.

But a single measurement of the projectile energy in the final state can determine whether or not the target has been excited. Therefore it seems sensible to consider the previous terms P_X and P_X^e to represent the probability that the target has been excited to any excited state. In that case, the expressions for the scattering entropy of Eqs. (17) and (36) can be thought of as general measures of entanglement for any projectile-target system that involves inelastic excitation.

High-energy proton-proton scattering. Data for total cross sections and total elastic cross sections are available from the Particle Data Group [35]. Then, the high-energy analysis presented above can be used with the identifications: $P_G = \sigma_{el}/\sigma_{tot}$, $P_X = 1 - P_G$ along with Eq. (36). The results are shown in Fig. 4.

At low energies there is no inelastic scattering, so the scattering entropy must vanish. This result is similar to the results shown in Fig. 1 for small values of k and to Fig. 2 for small values of u . As energies rise above inelastic scattering thresholds the entanglement increases. At still higher energies

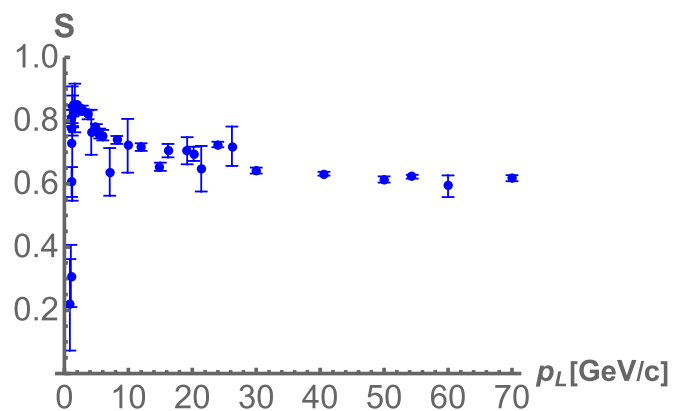


FIG. 4. S^e as a function of the fixed-target laboratory momentum p_L . The error bars reflect the uncertainties in reported cross sections [35].

the ratio of elastic to total cross sections is approximately flat. The entanglement entropy is substantial at laboratory momenta greater than about 2 GeV/ c (kinetic energy about 1.3 GeV). At higher energies than are shown, S is approximately flat with energy because the ratio σ_{el}/σ_{tot} is approximately independent of energy.

The large value of entanglement entropy indicates that the total absorption and gray disk models are reasonable

first approximations to understanding the data. The net result is that computing the scattering entropy provides insight regarding the underlying dynamics of proton-proton scattering and more generally that of projectile-target scattering.

Acknowledgment. This work was supported by the U.S. Department of Energy Office of Science, Office of Nuclear Physics under Award No. DE-FG02-97ER-41014.

-
- [1] P. J. Ehlers, Entanglement between valence and sea quarks in hadrons of 1+1 dimensional QCD, *Ann. Phys.* **452**, 169290 (2023).
- [2] D. E. Kharzeev and E. M. Levin, Deep inelastic scattering as a probe of entanglement, *Phys. Rev. D* **95**, 114008 (2017).
- [3] X. Feal, C. Pajares, and R. A. Vazquez, Thermal behavior and entanglement in Pb-Pb and p - p collisions, *Phys. Rev. C* **99**, 015205 (2019).
- [4] E. Gotsman and E. Levin, High energy QCD: Multiplicity distribution and entanglement entropy, *Phys. Rev. D* **102**, 074008 (2020).
- [5] M. Hentschinski, K. Kutak, and R. Straka, Maximally entangled proton and charged hadron multiplicity in deep inelastic scattering, *Eur. Phys. J. C* **82**, 1147 (2022).
- [6] R. Wang and X. Chen, Valence quark distributions of the proton from maximum entropy approach, *Phys. Rev. D* **91**, 054026 (2015).
- [7] S. R. Beane and P. J. Ehlers, Chiral symmetry breaking, entanglement, and the nucleon spin decomposition, *Mod. Phys. Lett. A* **35**, 2050048 (2019).
- [8] S. R. Beane, D. B. Kaplan, N. Klco, and M. J. Savage, Entanglement suppression and emergent symmetries of strong interactions, *Phys. Rev. Lett.* **122**, 102001 (2019).
- [9] Q. Liu, I. Low, and T. Mehen, Minimal entanglement and emergent symmetries in low-energy QCD, *Phys. Rev. C* **107**, 025204 (2023).
- [10] G. A. Miller, Entanglement maximization in low-energy neutron-proton scattering, [arXiv:2306.03239](https://arxiv.org/abs/2306.03239).
- [11] D. Bai, Spin entanglement in neutron-proton scattering, *Phys. Lett. B* **845**, 138162 (2023).
- [12] D. Bai and Z. Ren, Entanglement generation in few-nucleon scattering, *Phys. Rev. C* **106**, 064005 (2022).
- [13] C. W. Johnson and O. C. Gorton, Proton-neutron entanglement in the nuclear shell model, *J. Phys. G* **50**, 045110 (2023).
- [14] A. T. Kruppa, J. Kovács, P. Salamon, and Ö. Legeza, Entanglement and correlation in two-nucleon systems, *J. Phys. G* **48**, 025107 (2021).
- [15] A. T. Kruppa, J. Kovács, P. Salamon, Ö. Legeza, and G. Zaránd, Entanglement and seniority, *Phys. Rev. C* **106**, 024303 (2022).
- [16] C. Robin, M. J. Savage, and N. Pillet, Entanglement rearrangement in self-consistent nuclear structure calculations, *Phys. Rev. C* **103**, 034325 (2021).
- [17] E. Pazy, Entanglement entropy between short range correlations and the Fermi sea in nuclear structure, *Phys. Rev. C* **107**, 054308 (2023).
- [18] A. Tichai, S. Knecht, A. T. Kruppa, Ö. Legeza, C. P. Moca, A. Schwenk, M. A. Werner, and G. Zarand, Combining the in-medium similarity renormalization group with the density matrix renormalization group: Shell structure and information entropy, *Phys. Lett. B* **845**, 138139 (2023).
- [19] C. Gu, Z. H. Sun, G. Hagen, and T. Papenbrock, Entanglement entropy of nuclear systems, [arXiv:2303.04799](https://arxiv.org/abs/2303.04799).
- [20] A. Bulgac, Entanglement entropy, single-particle occupation probabilities, and short-range correlations, *Phys. Rev. C* **107**, L061602 (2023).
- [21] A. Bulgac, M. Kafker, and I. Abdurrahman, Measures of complexity and entanglement in many-fermion systems, *Phys. Rev. C* **107**, 044318 (2023).
- [22] A. Cervera-Lierta, J. I. Latorre, J. Rojo, and L. Rottoli, Maximal entanglement in high energy physics, *SciPost Phys.* **3**, 036 (2017).
- [23] Y. V. Kovchegov and E. Levin, *Quantum Chromodynamics at High Energy*, Cambridge Monographs on Particle Physics, Nuclear Physics and Cosmology Vol. 33 (Cambridge University Press, Cambridge, UK, 2013).
- [24] H. Frauenfelder and E. M. Henley, *Subatomic Physics*, 2nd ed. (Prentice-Hall, Englewood Cliffs, NJ, 1991).
- [25] K. Gottfried, *Quantum Mechanics Volume I: Fundamentals* (CRC, Boca Raton, 2018).
- [26] A. N. Kamal and H. J. Kreuzer, Soluble two-channel problems in potential scattering, *Phys. Rev. D* **2**, 2033 (1970).
- [27] R. Peschanski and S. Seki, Entanglement entropy of scattering particles, *Phys. Lett. B* **758**, 89 (2016).
- [28] R. Peschanski and S. Seki, Evaluation of entanglement entropy in high energy elastic scattering, *Phys. Rev. D* **100**, 076012 (2019).
- [29] R. J. Glauber, *Lectures in Theoretical Physics* (Interscience, New York, 1959), Chap. 3, pp. 315–415.
- [30] J. S. Blair, Theory of elastic scattering of alpha particles by heavy nuclei, *Phys. Rev.* **95**, 1218 (1954).
- [31] T. E. O. Ericson, *Preludes in Theoretical Physics* (North Holland, Amsterdam, 1966), pp. 321–329.
- [32] A. Y. Abul-Magd and M. H. Simbel, The accuracy of the Inopin-Ericson theory of nuclear diffraction scattering, *Nucl. Phys. A* **148**, 449 (1970).
- [33] H. Cheng and T. T. Wu, *Expanding Protons: Scattering at High Energies* (MIT Press, Cambridge, MA, 1987).
- [34] S. Donnachie, H. G. Dosch, O. Nachtmann, and P. Landshoff, *Pomeron Physics and QCD*, Cambridge Monographs on Particle Physics, Nuclear Physics and Cosmology Vol. 19 (Cambridge University Press, Cambridge, UK, 2004).
- [35] R. L. Workman *et al.* (Particle Data Group), Review of particle physics, *Prog. Theor. Exp. Phys.* **2022**, 083C01 (2022).